INTERNATIONAL JOURNAL FOR NUMERICAL METHODS IN FLUIDS
Int. J. Numer. Meth. Fluids 2001; **36**: 329–349 (DOI: 10.1002/fld.137)

Remedies for artificial diapycnal mixing in a σ co-ordinated model of Tokyo Bay[1]

Akinari Kaneko*,[2]

The Institute of Japanese Union of Scientists and Engineers, Sendagaya, Shibuya, Tokyo, Japan

SUMMARY

False diapycnal mixing often occurs due to horizontal diffusion in the simulation of heat, salinity, or water quality in estuaries by using a σ co-ordinated ocean model. The Princeton ocean model (POM) is used as a basic σ co-ordinated model and is applied to Tokyo Bay. Only river discharges are introduced into the model as external forces. Two remedies recommended in the POM, Stelling's horizontal diffusion approximation, Huang's new diffusion formula, Song and Haidvogel's *s* co-ordinates, and Smolarkiewicz advection scheme have all been examined for suppressing the false diapycnal mixing. The conclusions are that the simultaneous use of POM's remedy and Stelling's approximation and the simultaneous use of POM's remedy and *s* co-ordinates are the most effective. Copyright © 2001 John Wiley & Sons, Ltd.

KEY WORDS: diapycnal mixing; horizontal diffusion; isopycnal; ocean model; sigma co-ordinate; stratified flow

1. INTRODUCTION

σ co-ordinate systems, which accurately represent the bottom topography, are used for various simulations of free surface flow and transport in estuaries and seas. However, the σ-transformed grids give rise to numerical problems when applied to steep topographies [1–11]. One important problem is the horizontal pressure gradient error, and another is the occurrence of diapycnal mixing of temperature and salinity in stratified flow due to horizontal diffusive fluxes. Quite a few papers dealing with the former problem exclusively have been presented so far [5–11], while only a few papers [1,3,4] concern the latter, despite the fact that it is as important as the former. This paper studies the latter problem. We focus on remedies for the diapycnal mixing due to horizontal diffusion. How changing of the scheme of diffusive terms has an effect on suppressing diapycnal mixing is also investigated.

* Correspondence to: 6-2-31 Nakamuraminami, Tsuchiura, Ibaraki 300-0843, Japan.
[1] This paper was presented at the 3rd Symposium on Environmental Fluid Mechanics, Japan, 1998, and at the 4th Symposium on Environmental Fluid Mechanics, Japan, 1999.
[2] E-mail: kaneko@frontier.esto.or.jp

Received November 1998
Revised November 1999

The diapycnal mixing is a mixing across an isopycnal surface, perpendicular to isopycnal mixing. It would be considered numerical and false if it were not much smaller than isopycnal mixing in a stratified flow case, and the prediction of the σ co-ordinated model would then be inconsistent with the observed results. Here, we neither consider large oceans nor a global scale as a modeling application, but an estuarine scale (< 100 km). An isopycnal surface is perpendicular to the vertical direction in such a small region when flow is stratified. We do not deal with a slanted isopycnal surface. 'Diapycnal mixing' denotes 'vertical mixing' here. We treat numerical diffusive diapycnal mixing due to σ co-ordinates, which has no relation to isopycnal diffusion [12,13] in slanted isopycnal surface in Cartesian co-ordinates.

Horizontal diffusion problems in σ co-ordinate systems are explained by Mellor and Blumberg [1]. Governing equations in a σ co-ordinate system are obtained by co-ordinate transformation. However, horizontal diffusive terms are not transformed similarly since full σ-transformed horizontal diffusion is physically incorrect near sloping bottoms. This is because the conventional definition of horizontal diffusion, even in Cartesian co-ordinates, is physically incorrect. A net flux component normal to the bottom is too large in a numerical experiment. These are discussed in detail in Reference [1]. Therefore, they are transformed into a σ co-ordinate system, neglecting higher-order terms. That is to say, the same terms as in Cartesian co-ordinates remain. But then another problem appears instead. This is the numerical diapycnal mixing due to horizontal diffusion in a vertically changing σ co-ordinate surface, which is illustrated in Figure 1. The figure shows an ideal situation, where spurious diapycnal mixing occurs due to horizontal diffusion over a slanted topography. Isothermal lines are horizontal, shown as dotted lines, and temperature is vertically stratified. σ co-ordinate surfaces (solid lines) are slanted corresponding to the bottom topography and horizontal diffusion transport heat along the co-ordinate surface. The diffusion thus crosses the isotherm and then mixing takes place. The mixing makes the temperature uniform vertically and destroys the stratification.

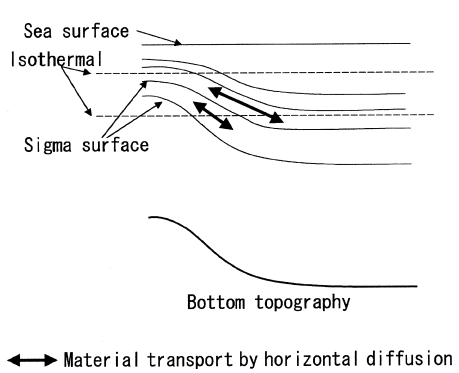

Figure 1. Numerical diapycnal mixing due to horizontal diffusion.

The false diapycnal mixing occurring in the stratified flow of Tokyo Bay is analyzed in this paper. Tokyo Bay has a steep topography and $\delta H/\delta x$ or $\delta H/\delta y$ is large. Accordingly, σ surfaces change vertically, as in Figure 1. It is thus anticipated that diapycnal mixing usually occurs in stratified flow if a σ co-ordinate model is applied to Tokyo Bay. Some studies [3,4] are careful about the 'hydrostatic consistency' $|\sigma/H\,\partial H/\partial x|\delta x < \delta\sigma$. It is seldom satisfied in the original topography under our calculation conditions. Most of the σ levels are 'hydrostatic inconsistent' at shallow regions near coasts, where the depth, H, is small (less than about 20 m), since $\partial H/\partial x$ is large, then $\delta H/H$ is large.

There are remedies proposed for this problem. Mellor and Blumberg [1,2] suggested a simple new formulation. Stelling and Kester [3] proposed an algorithm for the approximation in σ co-ordinates based on a finite volume method. A new formula for diffusive terms, which is different from the ordinary one, was presented by Huang and Spaulding [4]. Song and Haidvogel [14] showed that their s co-ordinates were useful for the application to a tall seamount topography. s co-ordinate systems may not be said to be one of the remedies, but one can say it includes the effect of reducing problems due to horizontal diffusion.

A model used for the analysis is described in the next section. The model is based on the Princeton ocean model (POM) [2,15]. In Section 3, simulation conditions, including initial and boundary conditions, are explained. Reference results using a Cartesian co-ordinate model are shown in Section 4. Six remedies are explained in Section 5. Most of them are related to horizontal diffusion, although the Smolarkiewicz advection scheme is examined as an example indirectly related to it. Numerical results for them are presented then. Section 6 contains some concluding remarks.

2. MODEL

The POM [2,15] is used here as a basic model and the main feature is as follows:

1. σ co-ordinated
2. mode splitting (three-dimensional internal mode and two-dimensional external mode)
3. second-order accuracy (leap frog and central difference advection scheme)
4. Mellor and Yamada turbulence closure model

POM is coupled with boundary subroutines developed by the present authors [16,17]. They make it possible to deal with the following boundary conditions:

1. breakwater (line land with no area)
2. non-slip, half a slip, or free slip condition for velocity along coast line
3. discharging water given by input data, without the loss of flow balance

However, (1) and (2) do not affect the results of this paper since breakwaters are not set in the numerical tests near where we watch in this paper, and lateral slip conditions are not important. The module size of this new POM is 2.5 times that of the original. The new POM is a little computationally expensive though [16]!

A remedy recommended in the POM for horizontal pressure gradient errors will be used for all numerical tests hereafter. That is, to subtract ρ_{mean} from a density before calculating

horizontal pressure gradient, where ρ_{mean} is the initial density field which is area-averaged on z-levels and then transformed to σ co-ordinates [2,6]. In Section 5 (remedies' tests in this paper), this new POM is modified and used in order that remedies for diapycnal mixing due to horizontal diffusion work properly in numerical tests.

3. SIMULATION CONDITIONS

Calculation conditions for the hydrodynamic analysis are listed in Table I. Constant horizontal eddy diffusivity is determined based on the observational data [18]. Constant eddy viscosity is determined so that the absolute value of surface velocity in the center of Tokyo Bay may become the same order of the observational data when the model includes winds and tides [16], since the larger the viscous energy, the less the kinetic energy, and the adjustment of viscous energy, i.e. viscous coefficients are used in order to adjust the velocity. In summer time, stratification is often forms in Tokyo Bay, and the temperature and salinity of the water are used as initial conditions after area averaging of the observational data. These vertical profiles of temperature and salinity are shown in Figure 2. Because spurious diapycnal mixing is focused upon and true diapycnal mixing due to tides and winds might obscure this, only river flows are considered as external forces. In this simulation, water with a high temperature and very low salinity flows from the rivers into Tokyo Bay and keeps flowing on the surface without submerging. Therefore, it is anticipated that flow is stratified and that real diapycnal mixing never occurs.

4. REFERENCE RESULTS

For comparison with σ co-ordinate models, reference results are obtained by using a Cartesian co-ordinate model that is different from that explained in Section 2. The model is a three-dimensional hydrostatic model using Cartesian co-ordinates, where mode splitting is not

Table I. Calculation conditions.

Grid size	Horizontal—400 m × 400 m Vertical—21 levels at every point (31 levels are partly used)
Eddy viscosity	Horizontal—50 $m^2 s^{-1}$ (if Smagorinsky coefficient is not used) Vertical—10^{-3} $m^2 s^{-1}$
Eddy diffusivity	Horizontal—10 $m^2 s^{-1}$ (if Smagorinsky coefficient is not used) Vertical—10^{-4} $m^2 s^{-1}$
Simulation time	60 h
Initial salinity and temperature	Area averaged prior to transfer to σ co-ordinates (observed values in summer are used)
Rivers	15 large rivers (the amounts of the flowing water, temperature, and salinity in summer are used)
Tidal currents	Not considered
Winds	Not considered

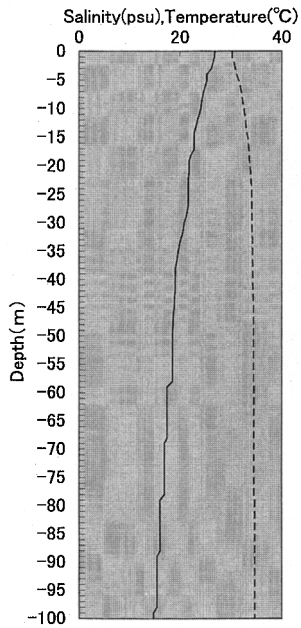

Figure 2. Initial vertical distributions of salinity and temperature. A solid line and a broken line denote temperature and salinity respectively.

used. The maximum number of vertical discretization is 21 near the bay mouth and the minimum vertical spacing is 1 m. The simulation conditions are the same as in Section 3.

The surface velocity fields by this model are shown in Figure 3. The magnitude of the velocity is small since the tidal current is not considered. In the dashed line area, westward flow from the Murata river collides with the southward flow from Naka, Ara, Edo rivers, and then it is considered that stratified flows are susceptible to be smeared there. Besides that, the area is in shallow water and the bottom topography is steep near the coast ($\delta H/\delta x$ is large). Hydrostatic consistency is not satisfied there since $\delta H/H$ is large. Therefore, this cross-section is a suitable area for investigating diapycnal mixing. Figure 4 shows a cross-sectional view of velocity fields along the dashed line in Figure 3, where the Cartesian co-ordinate model has the maximum 13 vertical levels at about 20 m depth.

In this figure, and all the figures of cross-sectional view hereafter, vertical velocities are magnified by $200\times$. Vertical velocity in a cross-section across Tokyo Bay (Figure 3) is used as an indicator of numerically spurious model behavior. Since vertical velocity is typically several orders of magnitude smaller than horizontal velocity, for presentation purposes it has been scaled by a factor 200 (i.e., velocities u, v and 200ω are plotted.) This scaling value is equal to the ratio of the sizes of a horizontal grid cell to a typical vertical grid cell and therefore the vectors roughly represent the relative sizes of horizontal and vertical fluxes throughout the cross-section.

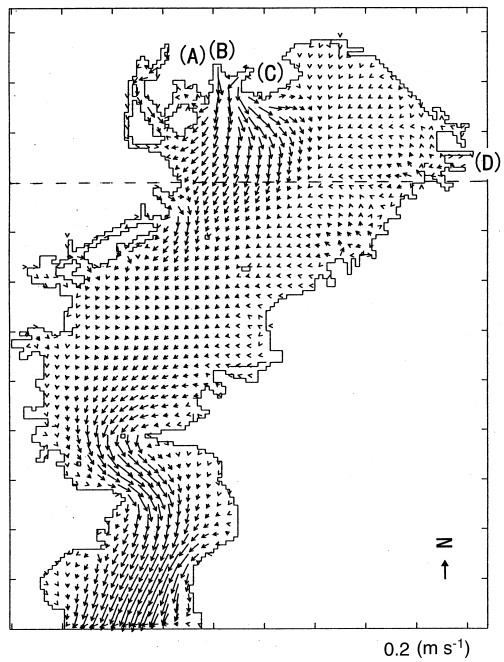

Figure 3. Surface velocity fields in the region of Tokyo Bay. Calculation conditions are listed in Table I. Cartesian co-ordinates are used. (A) Naka river, (B) Ara river, (C) Edo river, (D) Murata river.

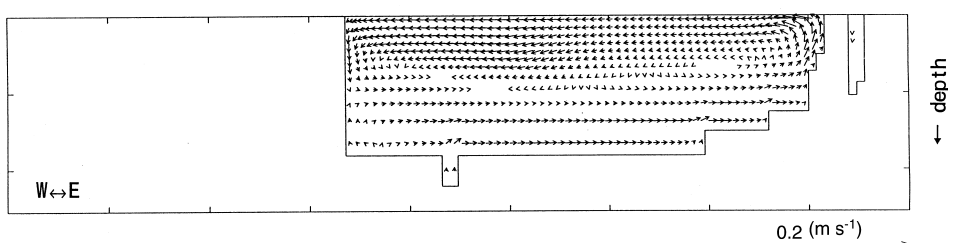

Figure 4. A cross-sectional view of velocity fields (Cartesian co-ordinates).

Stable and stratified fields are obtained after 60 h of simulation and no circulation is seen in Figure 4. Because the z co-ordinate surface is horizontal and does not vary vertically, spurious diapycnal mixing due to horizontal diffusion never happens. It is considered that these results almost represent the real phenomenon.

However, one can find a drawback of the Cartesian co-ordinates in Figure 4 even in this situation. A vertical flow appears in a hollow in the figure. This is not physically true and is considered due to the vertical wall of the bottom topography.

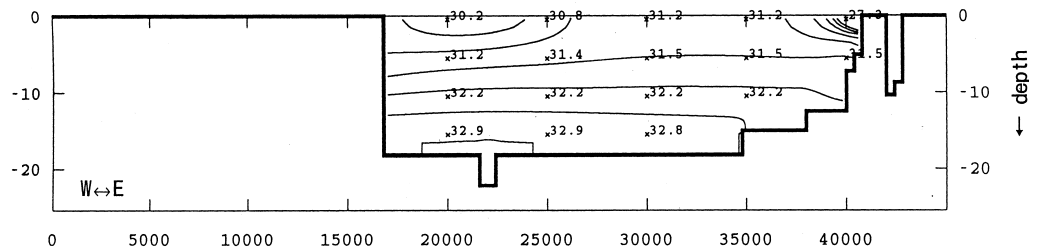

Figure 5. A cross-sectional view of salinity fields (Cartesian co-ordinates). A contour interval is 0.5 practical salinity units (psu).

Vertical salinity distribution is shown in Figure 5. Stratified fields are obtained corresponding to Figure 4. However, salinity fields are a little unstable under these numerical conditions because water with low salinity continues to flow into the bay. Estuarine water becomes diluted gradually. For this reason, salinity distribution is regarded as less important than velocity fields. However, even velocity fields become unstable after long hours of simulation due to the influence of changing salinity fields. It can be said that velocity fields have been in a stable state for a certain period. Whether velocity fields reach stable states or not is examined by flow balance, which is the ratio of the total amount of outflow from the baymouth per unit time to the total amount of inflow from the rivers per unit time. It becomes about 0.95–0.97 in 60 h of simulation in all the results in this paper. This means it is barotropically stable, and, in addition, it is also baroclinically stable because the maximum of the velocity difference during one δt is 0.006 cm s^{-1} in all of the computational domain after 60 h computation, and this is only 0.6 per cent of the average velocity.

5. REMEDIES AND RESULTS

5.1. Remedies based on the POM [1,2]

If all the horizontal diffusion terms after σ transformation are incorporated into the governing equations, diffusion in the simulation leads to physically incorrect results when bottom topographic slopes are large. A new formulation is to omit several terms of the transformation and keep the same terms as in Cartesian co-ordinate system.

$$Q_{xx+yy} = \frac{\partial}{\partial x}\left(A_{\mathrm{H}}\frac{\partial S}{\partial x}\right) + \frac{\partial}{\partial y}\left(A_{\mathrm{H}}\frac{\partial S}{\partial y}\right) \tag{1}$$

where S is the salinity or temperature, A_{H} the horizontal diffusivity, and Q_{xx+yy} the diffusion terms.

However, this brings about diapycnal mixing due to the vertical change of the σ co-ordinate surface instead. Two remedies for the diapycnal mixing are proposed.

(a) Subtraction of an area-averaged temperature (or salinity) or climatologies (reliable observed values), before the calculation of the diffusion terms.
(b) Use of Smagorinsky diffusivity (A_H)

$$A_M = A_{M0} + C\Delta x\Delta y\left(\left(\frac{\partial u}{\partial x}\right)^2 + \left(\frac{\partial v}{\partial x} + \frac{\partial u}{\partial y}\right) + \left(\frac{\partial v}{\partial y}\right)^2\right)^{1/2} \tag{2}$$

$$A_H = A_M/5.0 \tag{3}$$

where A_M is Smagorinsky viscosity and we use $A_{M0} = 10\ m^2\,s^{-1}$ based on Reference [19]. These are explained in Reference [2]. Here, a detailed explanation is attached in Appendix A. We use area-averaged initial temperature and salinity as 'climatologies' for (a) here.

Firstly, a numerical test without any remedies is carried out. The surface velocity fields are not shown here since it is almost the same as in Figure 3 (Cartesian co-ordinates). It also makes only a small difference in surface velocity fields whether any remedy is applied or not; accordingly no surface velocity fields will be illustrated hereafter. The results of the cross-section are given in Figure 6 (velocity fields) and Figure 7 (salinity fields). A lot of strong vertical circulation of flow is seen in Figure 6, which is considered due to false diffusion from the horizontal diffusion over the steep topography. False diffusion of temperature and salinity produces vertical velocities. False diffusion is considered to destroy temperature and salinity fields, to make them uniform vertically (Figure 1), and to construct horizontally unbalanced

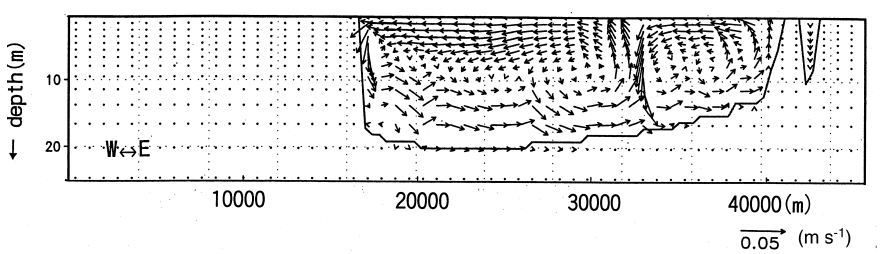

Figure 6. A cross-sectional view of velocity fields (no remedy).

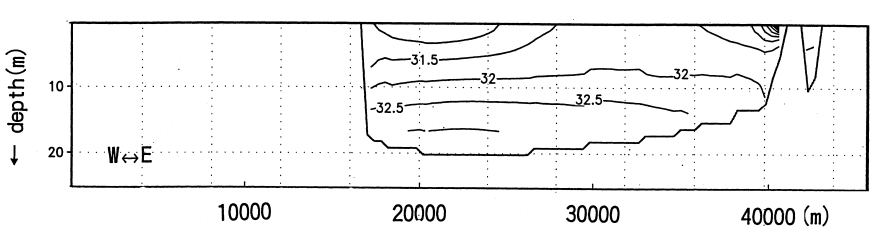

Figure 7. A cross-sectional view of salinity fields (no remedy). A contour interval is 0.5 psu.

density fields (pressure gradient force) through the Joint Panel of Oceanographic Tables and Standards (UNESCO) equation of state. This unstable density field is supposed to reduce (or sometimes produce) horizontal velocities through equations of motion and produce false vertical velocities through equations of continuity. Also, they would not be found if the vertical velocity were not magnified by 200.

Contour line salinity equaling 31.5 reaches the surface in the center of Figure 7, and the upwelling that salinity in the middle layer raises to the surface is considered numerical, i.e., false, since river discharges spread on the surface and the stratification is not considered to be destroyed then. Circulations in Figure 6 and upwelling in Figure 7 are considered related to the treatment of horizontal diffusive terms. This is explained in Figure 8 (velocity fields), where no remedy is applied with null diffusion. There is no circulation and it is almost the same as Figure 4. It is obvious that there would be no spurious diapycnal mixing if it were not for horizontal diffusion. However, it is actually known that a model with null diffusion does not give consistent results with the observation when tides and winds are taken into account. Predicted distributions of temperature and salinity are not smooth when compared with this observation. Therefore, null diffusion is impossible for the real application and horizontal diffusion is required to be equal to about 10 $m^2 s^{-1}$. We inevitably introduce remedies for diapycnal mixing. The remedies of the POM will be examined in the first.

A test with the above remedy (a) has been tried. The results are given in Figure 9 (velocity fields) and Figure 10 (salinity fields). Strong circulations are reduced here in comparison with

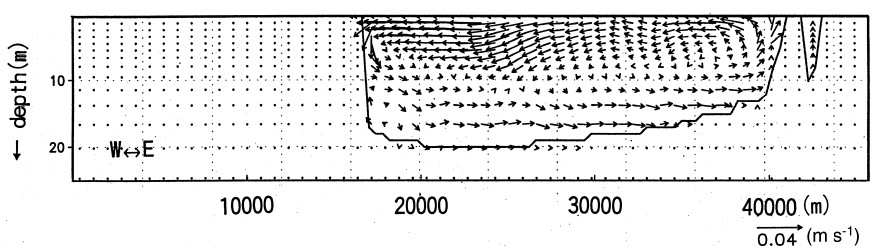

Figure 8. A cross-sectional view of velocity fields (null diffusion).

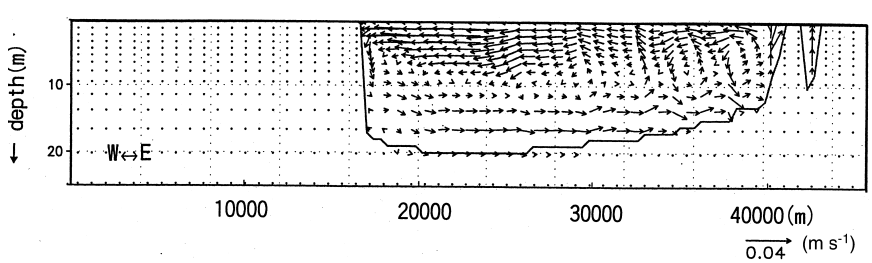

Figure 9. A cross-sectional view of velocity fields [Section 5.1 (a)].

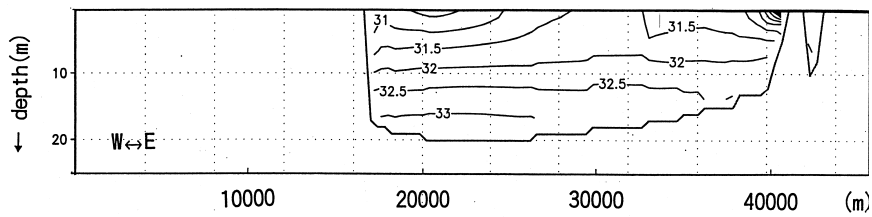

Figure 10. A cross-sectional view of salinity fields [Section 5.1 (a)]. A contour interval is 0.5 psu.

Figure 6. The area of salinity ≥ 31.5 on the surface in Figure 10 is smaller than that in Figure 7. The figures show remedy (a) is effective on suppressing false diapycnal mixing. However, a couple of vertical circulations of flow is seen in eastern areas of Figure 9, where the bottom is slanted ($\delta H = 2$ m, $\delta H/\delta x = 0.005$ and $H = 14$ m, i.e., $\delta H/H = 0.14$ is maximum here. This means the lower half of the water column is hydrostatically inconsistent.). This shows the σ co-ordinate model with remedy (a) is inferior to the Cartesian co-ordinate model with regard to the occurrence of spurious diapycnal mixing.

Both remedies (a) and (b) have been applied. Smagorinsky diffusivity and Smagorinsky viscosity are used here. In this test, eventually, velocities are small in the cross-section and A_M, A_H become $A_{M0} = 10\ \mathrm{m^2\,s^{-1}}$, $A_{M0}/5 = 2\ \mathrm{m^2\,s^{-1}}$ respectively. Therefore, the test becomes equivalent to one with remedy (a) and small horizontal diffusivity rather than Smagorinsky coefficients. The results are illustrated in Figure 11 (velocity fields) and Figure 12 (salinity fields). Since two small circulations in the eastern area, where the slope is slanted, almost disappear in Figure 11, it can be said that more improved stratification is obtained there than in Figure 9, although it is not clear in Figure 12. It has been shown that using both remedy (a) and the small horizontal coefficients is more effective on false diapycnal mixing than using just remedy (a). Consequently, to use remedy (b) in addition to (a) is also expected to be effective.

The dependence of vertical resolution on the occurrence of spurious diapycnal mixing has been investigated. Tests with just remedy (a) and without any remedy have been tried with 31

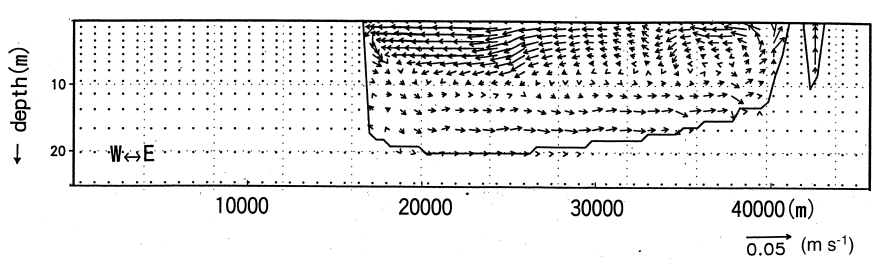

Figure 11. A cross-sectional view of velocity fields [Section 5.1 (a) and (b)].

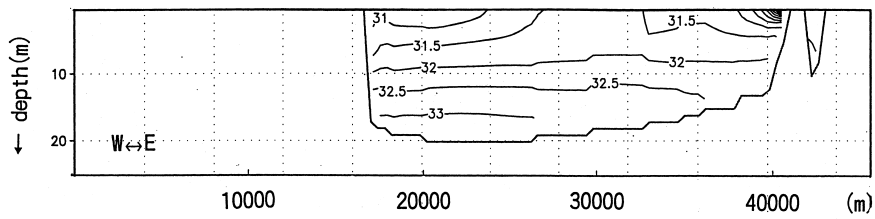

Figure 12. A cross-sectional view of salinity fields [Section 5.1 (a) and (b)]. A contour interval is 0.5 psu.

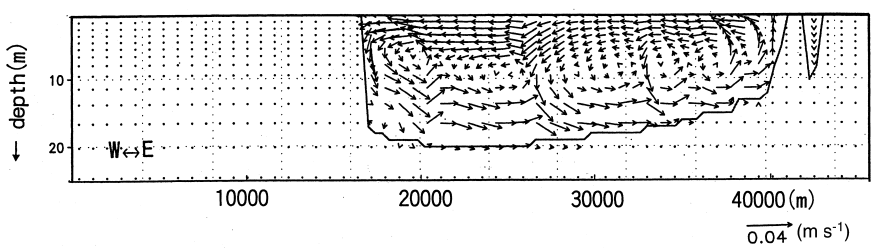

Figure 13. A cross-sectional view of velocity fields (no remedy, vertical levels = 31).

vertical levels, while there are 21 in Figures 6 and 9. The results are shown in Figure 13 (no remedy) and Figure 14 (remedy (a)). In Figure 13, flow in upper layers near the sea surface is improved since the vertical change of uppermost layers becomes smaller than in Figure 6, even over steep topography.

Figure 14 almost coincides with Figure 9. This indicates that to increase vertical levels does not improve the false model behavior, and 21 vertical levels are sufficient for model prediction if remedy (a) is used. This coincidence also gives evidence for the model convergence.

Not only are horizontal diffusion and pressure gradient considered causes of the diapycnal mixing, but also the numerical scheme for salinity or temperature is considered. The central

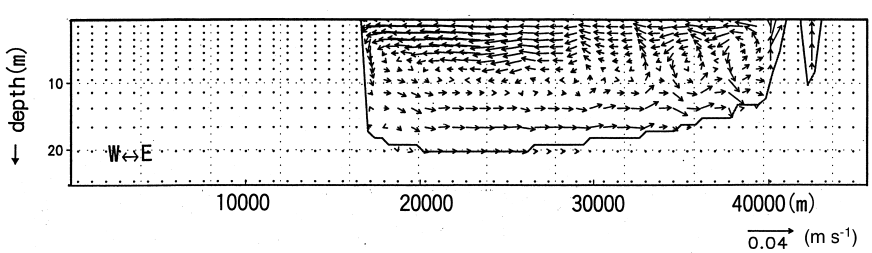

Figure 14. A cross-sectional view of velocity fields [Section 5.1 (a), vertical levels = 31].

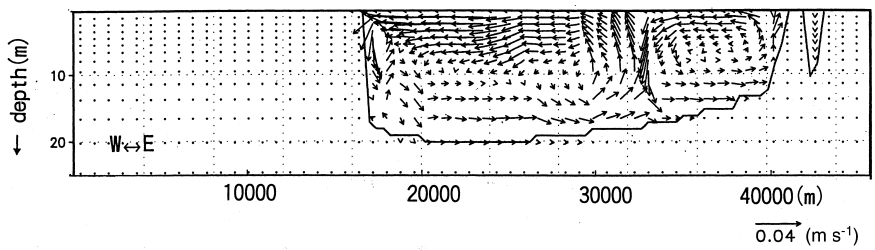

Figure 15. A cross-sectional view of velocity fields (Section 5.2).

difference advection scheme is used in the POM. Problems with the central difference are reported in Reference [20], and therefore the Smolarkiewicz upwind scheme [21,22] has been tried as a vertical advection scheme for salinity and temperature. The upstream advection scheme preserves the positive definite property, but the numerical schemes with the first-order approximation lead to excessive numerical diffusion. In the Smolarkiewicz scheme, this effect is compensated for by introducing an additional time level of numerical computations. The results using the vertical advection scheme for temperature and salinity and remedy (a), which are not shown here, almost coincide with Figures 9 and 10. This suggests that the application of the Smolarkiewicz scheme to vertical advection instead of the central difference does not affect diapycnal mixing.

5.2. A remedy by Stelling and Kester [3]

Stelling and Kester proposed an algorithm for the approximation in σ co-ordinates of the horizontal diffusive fluxes of temperature and salinity, based on a finite volume method. This remedy is equivalent to the horizontal diffusive terms being computed in Cartesian co-ordinates and the other terms in σ co-ordinates. Diffusive terms used are the same as Mellor and Blumberg's (Section 5.1). Here, control volumes are reconstructed for diffusive fluxes in order that the x, y grid lines are perpendicular to vertical ones and that the consistent approximation of the horizontal diffusive fluxes and minimal artificial vertical diffusion are obtained.

The algorithm is tested by the first test for a horizontal diffusion in Reference [3], and the test results (not shown here) almost coincide with those of Reference [3]. It is anticipated that horizontal diffusion will never lead to diapycnal mixing over a slope topography.

The calculation results in Tokyo Bay as in Section 5.1 are shown in Figure 15 (velocity fields) and in Figure 16 (salinity fields). They show that a large vertical circulation of flow is seen in the center of the figures but there is no diapycnal mixing over the sloping bottom in the eastern area of the figures. The latter good results are consistent with the results of the simple test in Reference [3]. The reason for the former problem is not clear. It is considered related to the grid size, the uneven bottom, and the collision of the two river flows. It may be also possible that the remedy does not work well because of insufficient vertical resolution. We have tried the remedy with fine vertical resolution (the number of vertical levels = 31). The velocity fields are shown in Figure 17. The large vertical circulation in Figure 15 almost

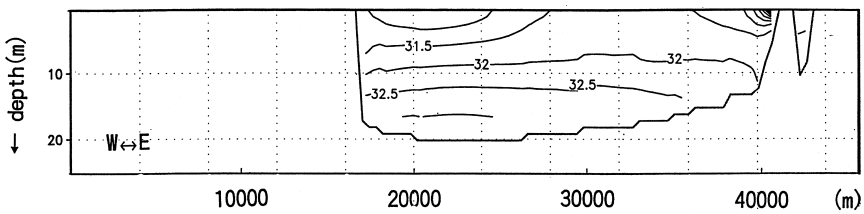

Figure 16. A cross-sectional view of salinity fields (Section 5.2). A contour interval is 0.5 psu.

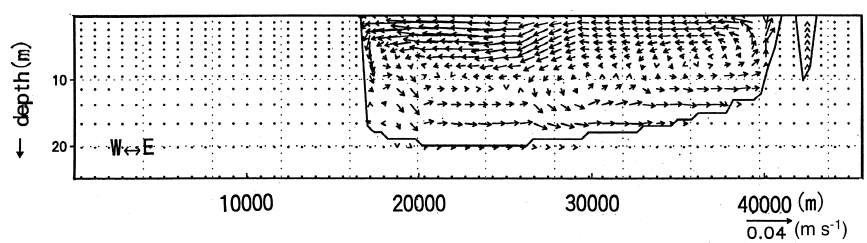

Figure 17. A cross-sectional view of velocity fields (Section 5.2, vertical levels = 31).

disappears, although undesirable submerging flow remains in the center of the figure and the result is almost acceptable. This remedy is understood to be promising.

Next, consider remedy (a) in Section 5.1 with the remedy in this subsection together. The vertical resolution is 21. There is no theoretical reason for denying the simultaneous use of both the remedies. The velocity fields results (Figure 18) illustrate that non-smeared stratified

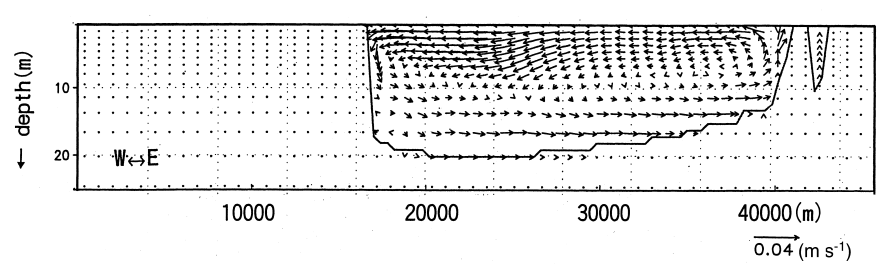

Figure 18. A cross-sectional view of velocity fields [Section 5.2 and Section 5.1 (a)].

flow is obtained in the entire cross-section and that it is reproducing almost the same result as that in Figure 4, while avoiding problematic vertical flow in a hollow in Figure 4.

As a result, it has been shown that a combination of remedy (a) in Section 5.1 and the remedy by Reference [3] is very effective on suppressing diapycnal mixing due to horizontal diffusion.

5.3. A remedy by Huang and Spaulding [4]

A new formula for diffusive terms was presented by Huang and Spaulding. They use neither the same diffusive terms as in Sections 5.1 and 5.2, nor all the diffusive terms by the σ transformation. They use the same simple diffusive terms as in Cartesian co-ordinate system with an additional three terms, which are given below

$$Q_{xx+yy} = \frac{\partial}{\partial x}\left(A_{\mathrm{H}}\frac{\partial S}{\partial x}\right) + \frac{\partial}{\partial y}\left(A_{\mathrm{H}}\frac{\partial S}{\partial y}\right) - 2\frac{\partial}{\partial x}\left(\frac{A_{\mathrm{H}}\Psi_x}{H}\frac{\partial S}{\partial \sigma}\right) - 2\frac{\partial}{\partial y}\left(\frac{A_{\mathrm{H}}\Psi_y}{H}\frac{\partial S}{\partial \sigma}\right) + \left(\frac{A_{\mathrm{H}}\Psi_x^2 + A_{\mathrm{H}}\Psi_y^2}{H}\right)\frac{\partial}{\partial \sigma}\left(\frac{1}{H}\frac{\partial S}{\partial \sigma}\right) \tag{4}$$

where $\Psi = \sigma H(x, y)$, $\Psi_x = \sigma\, \partial H(x, y)/\partial x$, $\Psi_y = \sigma\, \partial H(x, y)/\partial y$, S is the salinity or temperature, H the depth, A_{H} the horizontal diffusivity, and Q_{xx+yy} the diffusion terms. The first two terms of Equation (4) are the original diffusion terms (1) in Cartesian co-ordinates, which are used as diffusion terms in Sections 5.1 and 5.2.

A model with these additional diffusion terms has been examined by the first simple test in Reference [3], as in Section 5.2. As a result, the model does not work and the stratification is destroyed. Complete mixing takes place then, but if the bottom slope is about 0.03, as recommended in Reference [4], the model works well and the stratification is formed.

The model has been applied to Tokyo Bay as in Sections 5.1 and 5.2, but it does not work on the original topography. Although Huang and Spaulding [4] reported that hydrostatic consistency is necessary for their model, it appears that $\partial H(x, y)/\partial x \ll 1$ (or $\partial H(x, y)/\partial y \ll 1$) is a necessary condition for their model since the diffusion terms (4) include lots of $\partial H(x, y)/\partial x$ and $\partial H(x, y)/\partial y$. Therefore, strong smoothing for topography is applied to Tokyo Bay in order that $\partial H(x, y)/\partial x$ and $\partial H(x, y)/\partial y$ become small. The topography after smoothing is shown in Figure 19, together with the original topography (Figure 20). It is hard to say the topography after smoothing is that of Tokyo Bay, but diapycnal mixing has been examined as in the previous subsections. The results are shown in Figure 21 (velocity fields) and in Figure 22 (salinity fields). They show that a large vertical circulation of flow is seen in the center of the figure. This is almost the same situation as in Section 5.2. Consider remedy (a) in Section 5.1 with the new diffusive terms in Reference [4] together. The velocity fields results (Figure 23) illustrate that stratified flow is obtained and that it is almost acceptable. Consequently, it has been shown that simultaneous use of remedy (a) in Section 5.1 and the new diffusive terms in this subsection affects suppressing diapycnal mixing due to horizontal diffusion, although the restriction on slope topography is sufficiently severe that this method may not be of practical value in many field applications.

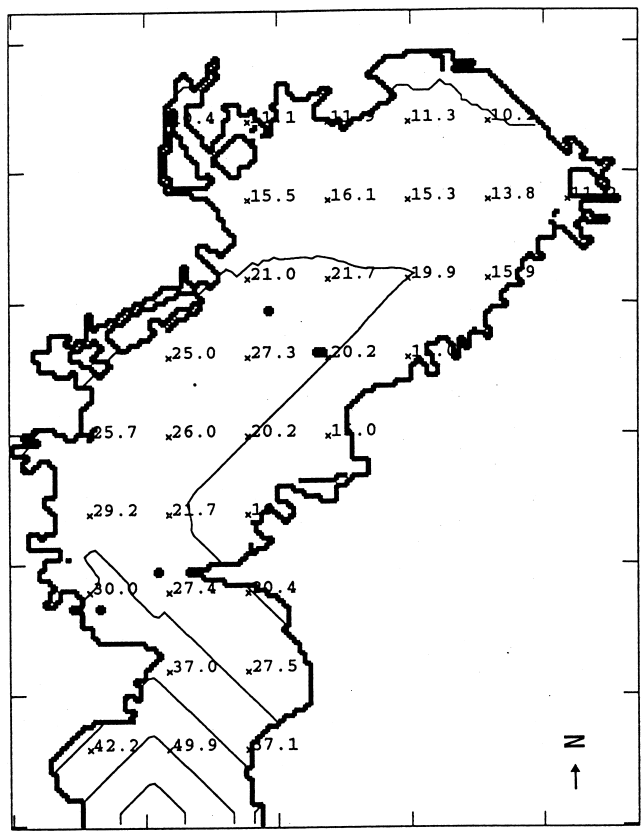

Figure 19. Topography after smoothing. A contour interval is 10 m.

5.4. A remedy by Song and Haidvogel [14] (s co-ordinate systems)

s co-ordinate systems have been proposed by several authors [14,23,24]. Song and Haidvogel [14] showed that their non-linear terrain following co-ordinates (*s* co-ordinates) had an effect on the application to a tall seamount topography, where a steep topography leads to numerical errors and instabilities. Although this paper is concerned with the improvement of problems due to horizontal diffusion, *s* co-ordinates are anticipated to improve diapycnal mixing due not only to horizontal diffusion but also to horizontal pressure gradient, and give interesting results in the cross-sectional view of velocity fields.

An *s* co-ordinated POM has been constructed here based on Song and Haidvogel [14]. A new co-ordinate '*s*' is expressed as follows:

$$z = \zeta(1+s) + h_c s + (h - h_c)C(s) \tag{5}$$

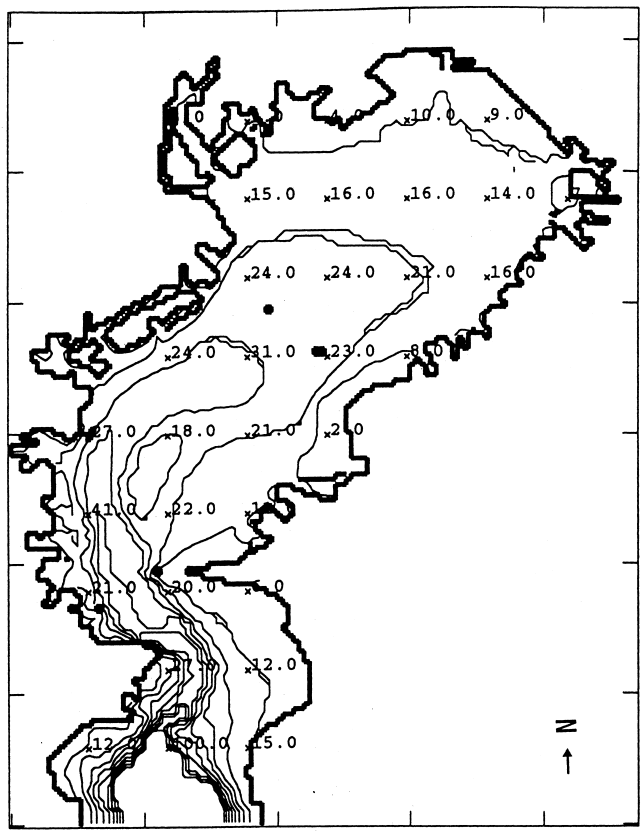

Figure 20. The original topography of Tokyo Bay. A contour interval is 10 m.

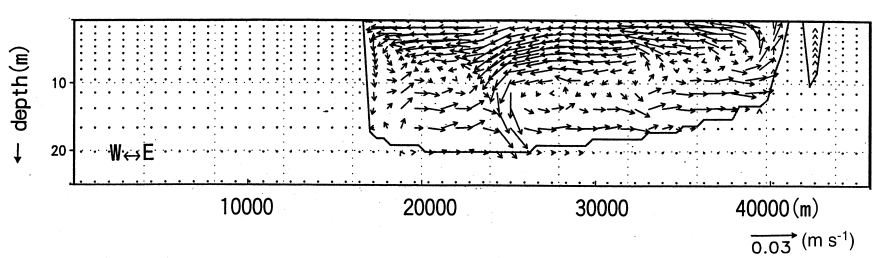

Figure 21. A cross-sectional view of velocity fields (Section 5.3).

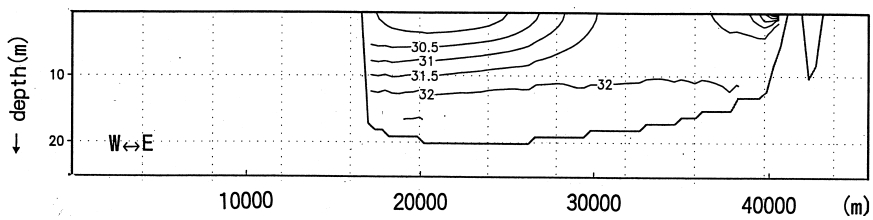

Figure 22. A cross-sectional view of salinity fields (Section 5.3). A contour interval is 0.5 psu.

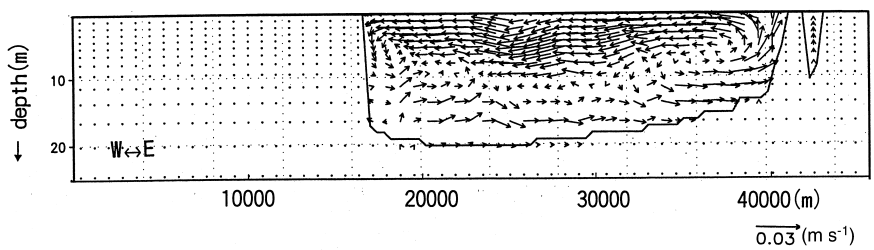

Figure 23. A cross-sectional view of velocity fields [Section 5.3 and Section 5.1 (a)].

$C(s)$ is defined as follows:

$$C(s) = (1-b)\frac{\sinh(\theta s)}{\sinh(\theta)} + b\frac{\tanh(\theta(s+1/2)) - \tanh((1/2)\theta)}{2\tanh((1/2)\theta)} \tag{6}$$

where ζ is the surface elevation, h the depth, h_c a constant chosen to be the minimum depth of the bathymetry, θ and b are surface and bottom control parameters and are set to 5 and 0.4 respectively.

The differences between σ co-ordinate and the s co-ordinate are shown in Figures 24 and 25, where the bottom slopes are expressed as a function $H(x) = -95/(\exp(6.296 \times 10^{-3}x) + 1) - 5$, $-1500 < x < 1500$. It is clear from these figures that z is a linear function of σ and a non-linear function of s. The change of the co-ordinate surface in σ co-ordinates is much larger than in s co-ordinates in upper layers.

A cross-sectional view of the results as in previous subsections is shown in Figure 26 (velocity fields) and Figure 27 (salinity fields) when the s co-ordinate model is applied to Tokyo Bay. Here, remedy (a) in Section 5.1 is also used. Figure 26 illustrates that much improved stratified flow is obtained, similar to Figure 4 although the flow near the bottom is a little problematic. Figure 27 also illustrates that contour line salinity equaling 31.5 does not reach the surface in the center of the figure and the upwelling is suppressed. The reason for the effect of the s co-ordinates is considered to be that an s surface near the sea surface does not vary much vertically, even if the depth varies steeply and that horizontal diffusion is then not

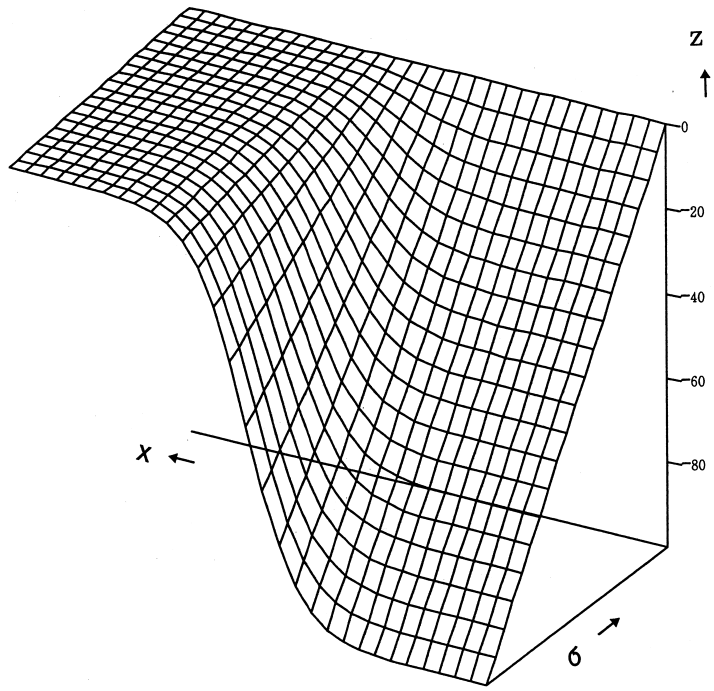

Figure 24. $z(x, \sigma)$ in σ co-ordinates. A bottom terrain function $H(x) = -95/(\exp(6.296 \times 10^{-3}x) + 1) - 5, \ -1500 < x < 1500$.

likely to produce diapycnal mixing, since the vertical component of the horizontal diffusion is very small. Non-slanted layers, i.e., layers changing little vertically, near the sea surface are effective, like a z co-ordinate surface, and these are not obtained by increasing the number of vertical levels (as in Section 5.1). Hence, these s co-ordinates are regarded as a combination of Cartesian co-ordinates in upper layers with σ co-ordinates in lower layers.

6. CONCLUSION

Although there are several causes considered for the spurious diapycnal mixing occurring in the σ co-ordinate model, the diapycnal mixing due to horizontal diffusion is analyzed by cross-sectional velocity fields with magnified vertical velocity. Vertical circulation of flow emerges in the cross-sectional view in the case of the presence of the diapycnal mixing. Six remedies for diapycnal mixing are examined and the following results on suppressing diapycnal mixing are obtained.

1. Two remedies recommended in the POM [One is (a) subtraction of an area-averaged value, the other is (b) a Smagorinsky diffusivity, explained in Section 5.1] are effective but not complete.

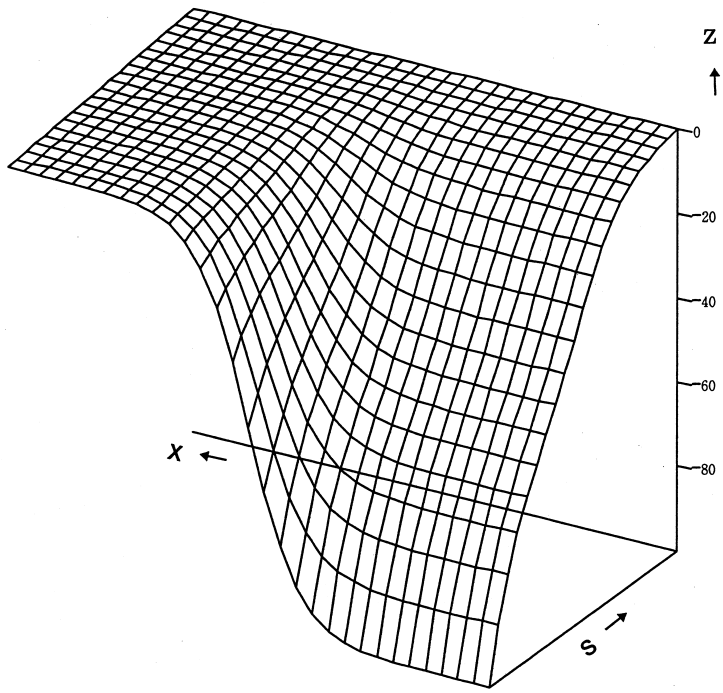

Figure 25. $z(x, s)$ in s co-ordinates. A bottom terrain function $H(x) = -95/(\exp(6.296 \times 10^{-3}x) + 1) - 5$, $-1500 < x < 1500$. Parameters $\theta = 5$, $b = 0.4$.

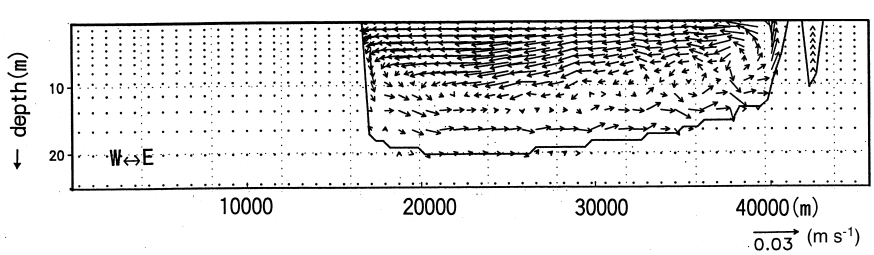

Figure 26. A cross-sectional view of velocity fields [Section 5.4 and Section 5.1 (a)].

2. Computational results are independent of vertical resolution if remedy (a) is introduced.
3. The Smolarkiewicz scheme for vertical advection for salinity or temperature equation is not effective at all.
4. Stelling and Kester's approximation for horizontal diffusive flux is effective, especially when vertical resolution is fine. It becomes almost complete with (a) in Section 5.1.

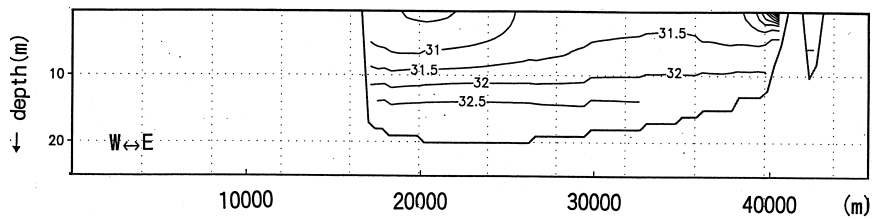

Figure 27. A cross-sectional view of salinity fields [Section 5.4 and Section 5.1 (a)]. A contour interval is 0.5 psu.

5. Huang and Spaulding's new formula with (a) in Section 5.1 requires strong smoothing of the topography to be effective and is therefore of limited practical value.
6. Song and Haidvogel's s co-ordinates, together with (a) in Section 5.1, are almost complete.

It is considered that the most recommended methods for suppressing diapycnal mixing are (4) and (6) above.

ACKNOWLEDGMENTS

The author is grateful to a large number of persons who contributed in various ways to the progress of the developmental work reported in this paper. He especially expresses his gratitude to Professor T. Matsuno for his valuable comments and suggestions. He also appreciates the valuable suggestions made by anonymous reviewers.

APPENDIX A

A.1. Explanation of Section 5.1(a)

This causes temperature or salinity to diffuse back to the observation (climatologies) rather than to a homogeneous values.

Consider a thermal flux 'q', 'q_{POM}' used in the calculation of temperature diffusion equation in σ co-ordinate system. 'q' is ordinarily defined as follows:

$$q = k(T_i - T_{i-1})/\Delta x \tag{A1}$$

where k is the thermal conductivity; Δx the grid spacing; T_i, T_{i-1} the temperature in horizontally adjacent cells in σ levels; and it is assumed that cell i is higher than cell $i-1$ in z levels. Accordingly, T_i may be higher than T_{i-1} (see Figure 1 to understand the situation).

For (a), q_{POM} is defined as follows:

$$q_{\mathrm{POM}} = k((T_i - T0_i) - (T_{i-1} - T0_{i-1}))/\Delta x \tag{A2}$$

where $T0_i$, $T0_{i-1}$ are the area-averaged temperature obtained from observation (climatologies).

Position i is closer to the sea surface than position $i-1$, then $T0_i > T0_{i-1}$.

In the ordinary case, i.e. Equation (A1), spurious diffusion tends to occur along σ surface from position i to position $i-1$. However, in the case of (a), i.e., Equation (A2), this spurious diffusion is reduced by $(T0_i - T0_{i-1})$. Thus, the application of (a) suppresses artificial diffusion.

A.2. Explanation of Section 5.1(b)

Horizontal velocity becomes small over steep topography; hence the space derivatives become small too. According to Equation (2), the value of the parentheses becomes small, A_H becomes small. Thus, Smagorinsky diffusivity suppresses artificial horizontal diffusion.

REFERENCES

1. Mellor GL, Blumberg AF. Modeling vertical and horizontal diffusivities with the sigma coordinate system. *Monthly Weather Review* 1985; **113**: 1379–1383.
2. POM. *Users Guide*, 1996. http://www.aos.princeton.edu/WWWPUBLIC/htdocs.pom [accessed March 1997].
3. Stelling GS, Van Kester JAThM. On the approximation of horizontal gradients in sigma co-ordinates for bathymetry with steep bottom slopes. *International Journal for Numerical Methods in Fluids* 1994; **18**: 915–935.
4. Huang W, Spaulding M. Modeling horizontal diffusion with sigma coordinate system. *Journal of Hydraulic Engineering* 1996; **122**: 349–352.
5. Haney RL. On the pressure gradient force over steep topography in sigma coordinate ocean models. *Journal of Physics and Oceanography* 1991; **21**: 610–619.
6. Mellor GL, Ezer T, Oey LY. The pressure gradient conundrum of sigma coordinate ocean models. *Journal of Atmospheric and Oceanic Technology* 1994; **11**: 1126–1134.
7. Mellor GL, Wang XH. Pressure compensation and the bottom boundary layer. *Journal of Physics and Oceanography* 1996; **26**: 2214–2222.
8. Mellor GL, Oey LY, Ezer T. Sigma coordinate pressure gradient errors and the Seamount problem. *Journal of Atmospheric and Oceanic Technology* 1998; **15**: 1122–1131.
9. McCalpin JD. A comparison of second-order and fourth-order pressure gradient algorithms in a σ-co-ordinate ocean model. *International Journal for Numerical Methods in Fluids* 1994; **18**: 361–383.
10. Chu PC, Fan C. Sixth-order difference scheme for sigma coordinate ocean models. *Journal of Physics and Oceanography* 1997; **27**: 2064–2071.
11. Slordal LH. The pressure gradient force in sigma co-ordinate ocean models. *International Journal for Numerical Methods in Fluids* 1997; **24**: 987–1017.
12. Redi MH. Oceanic isopycnal mixing by coordinate rotation. *Journal of Physics and Oceanography* 1982; **12**: 1154–1158.
13. Cox MD. Isopycnal diffusion in a z-coordinate ocean model. *Ocean Model* 1987; **74**: 1–5.
14. Song Y, Haidvogel D. A semi-implicit ocean circulation model using a generalized topography-following coordinate system. *Journal of Computational Physics* 1994; **115**: 228–244.
15. Blumberg AF, Mellor GL. A description of a three-dimensional coastal ocean circulation model. In *Three-dimensional Coastal Ocean Models*, Coastal Estuarine Science Series, vol. 4, Heaps NS (ed.). American Geophysical Union: Washington, DC, 1987; 1–16.
16. Kaneko A, Sueno M. Application of Princeton Ocean Model (POM) to Tokyo Bay. In *The Proceedings of the 74th JSME Spring Annual Meeting*, vol. III, 1997; 1753, 460 (in Japanese).
17. Kaneko A, Ino H. Application of Princeton Ocean Model (POM) to Tokyo Bay in fine resolution. In *The Proceedings of the 2nd Symposium on Environmental Fluid Mechanics*, 1997; D243, 501 (in Japanese).
18. Matsunashi J. *Kankyouryuutaiosen*. Morikita-Shuppan Press: Tokyo, 1993 (in Japanese).
19. Brooks DA. A model study of the buoyancy-driven circulation in the Gulf of Maine. *Journal of Physics and Oceanography* 1994; **24**: 2387–2412.
20. Pietrzak JD. A comparison of advection schemes for ocean modelling, Danish Meteorological Institute Scientific Report 95-8, 1995.
21. Smolarkiewicz PK. A simple positive definitive advection transport scheme with small implicit diffusion. *Monthly Weather Review* 1983; **111**: 479–486.
22. Smolarkiewicz PK. A fully multidimensional positive definitive advection transport algorithm with small implicit diffusion. *Journal of Computational Physics* 1984; **54**: 325–362.
23. Gerdes R. A primitive equation ocean circulation model using a general vertical coordinate transformation 1. Description and tesing of the model. *Journal of Geophysical Research* 1993; **98**: 683–701.
24. Mellor GL, Hakkinen S, Ezar T. A generalization of a sigma coordinate ocean model and an intercomparison of model vertical grids. In *Ocean Forecasting: Theory and Practice*, Pinardi N (ed.). Springer: Berlin, 2001.

